

UNCLASSIFIED

Defense Technical Information Center
Compilation Part Notice

ADP012389

TITLE: Spatially-Resolved Temperature Diagnostic for the Chemical Oxygen-Iodine Laser Based on a Variant of Saturation Spectroscopy

DISTRIBUTION: Approved for public release, distribution unlimited

This paper is part of the following report:

TITLE: Gas and Chemical Lasers and Intense Beam Applications III Held in San Jose, CA, USA on 22-24 January 2002

To order the complete compilation report, use: ADA403173

The component part is provided here to allow users access to individually authored sections of proceedings, annals, symposia, etc. However, the component should be considered within the context of the overall compilation report and not as a stand-alone technical report.

The following component part numbers comprise the compilation report:

ADP012376 thru ADP012405

UNCLASSIFIED

Spatially-resolved temperature diagnostic for the chemical oxygen-iodine laser based on a variant of saturation spectroscopy

Grady T. Phillips, Glen P. Perram, and Won B. Roh
Air Force Institute of Technology

ABSTRACT

The Chemical Oxygen-Iodine Laser (COIL) depends upon a supersonic mixing nozzle to produce optical gain on the $^2P_{1/2} - ^2P_{3/2}$ atomic iodine transition at $\lambda = 1.315 \mu\text{m}$. The translational temperature in the gain generator is particularly important, as the yield of singlet oxygen required to reach lasing threshold decreases from 17% at room temperature to 6% at $T=150\text{K}$. We have demonstrated an optical technique for measuring the gas temperature in the COIL supersonic expansion region with a spatial resolution of less than 12 mm^3 using a novel variant of saturated laser spectroscopy. The sub-Doppler hyperfine spectrum of the visible $\text{I}_2 X^1\Sigma_g^+ \rightarrow B^3\Pi(0_u^+)$ transition exhibits 15 or 21 transitions and has been recorded using laser saturation spectroscopy with a resolution of about 10 MHz. Pressure broadening of the hyperfine components and cross-relaxation effects have been studied and depend significantly on rotational level. By altering the saturation spectroscopy apparatus so that the pump and probe beams are nearly co-propagating, a Doppler profile, limited to the iodine sample in the volume of the overlapped beams, is obtained. Temperature, as derived from the Doppler profile, is spatially resolved and used to examine the flow from a small supersonic nozzle assembly.

Keywords: saturation spectroscopy, iodine, hyperfine spectrum, linewidth, pressure broadening, temperature diagnostic, Chemical Oxygen-Iodine Laser (COIL), cross-relaxation, velocity-changing collisions

1. INTRODUCTION

Since the first demonstration of a Chemical Oxygen-Iodine Laser (COIL) in 1978,¹ the technology has advanced significantly to supersonic laser devices with high output power and excellent beam quality.²⁻⁴ The Chemical Oxygen-Iodine Laser operates on the hyperfine components of the $5^2P_{1/2} - 5^2P_{3/2}$ transition in atomic iodine and is chemically pumped through energy transfer from the metastable $\text{O}_2(a^1\Delta)$. The $\text{O}_2(a^1\Delta)$ and $\text{I}(^2P_{1/2})$ states are nearly resonant with an energy defect of only 279 cm^{-1} . Several excellent reviews of the laser hardware, chemistry, laser physics, and fluid dynamics of these devices are available.²⁻⁴

The COIL device employs a supersonic mixing nozzle to: (1) inject, mix and dissociate molecular iodine to produce the lasant, atomic iodine, (2) produce a spatially uniform gain and a region of uniform index of refraction for good beam quality, (3) increase the laser power for a given flow cross-sectional area, and (4) reduce the gas temperature in the gain cavity. The translational temperature is particularly important for COIL, as the yield of singlet oxygen required to reach lasing threshold decreases from 17% at room temperature to 6% at $T=150\text{K}$.²

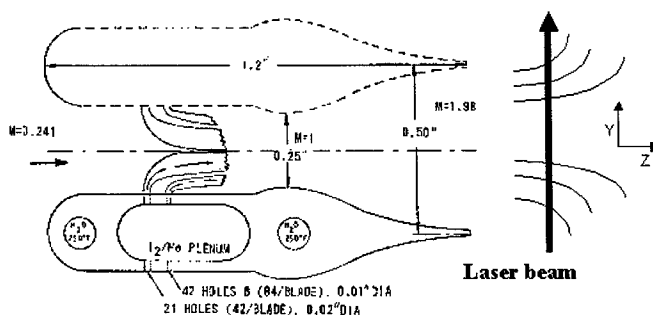


Figure 1. RotoCOIL mixing nozzle.²

Spatial distributions of the small signal gain and cavity temperature at the exit of the supersonic mixing nozzle of Chemical Oxygen-Iodine Lasers (COIL) have been measured previously by diode laser spectroscopy on the $^2P_{1/2}(F'=3) -$

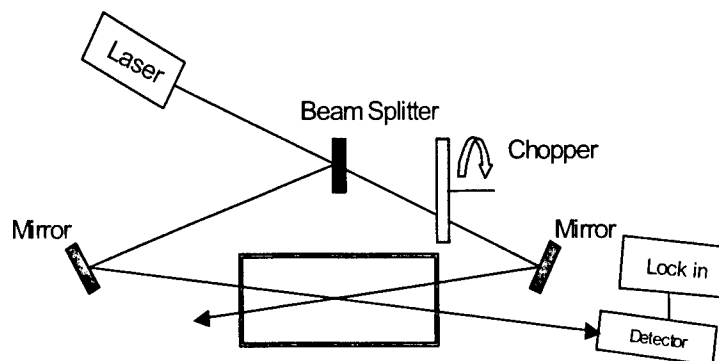
¹glen.perram@afit.edu; phone 1 937 255 3636 x 4504; Fax 1 937 255 2921; <http://www.afit.edu>; Air Force Institute of Technology/ENP, 2950 P Street, Wright-Patterson AFB, OH 45433-7765

$^2P_{3/2}(F=4)$ transition in atomic iodine.⁵ The resulting cavity temperatures of about 200 K is significantly higher than the predicted temperature of the supersonic expansion of about 150 K. The technique is limited to measuring an average temperature along the direction of the diode laser beam propagation and may be biased due to the directed flow resulting from symmetrical turbulent vortices, as illustrated in Figure 1. An optical technique for measuring the three-dimensional temperature flow field at the exit plane of the supersonic nozzle is required to fully assess nozzle efficiency and chemical heat release during I_2 dissociation. The focus of the present work is to exploit a novel variant of laser saturation spectroscopy to develop a temperature diagnostic with spatial resolution of less than 12 mm^3 .

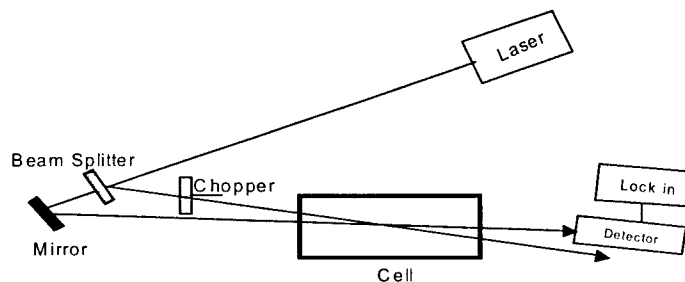
2. EXPERIMENT

Laser saturation spectroscopy is a well established technique for obtaining sub-Doppler resolution in gas phase spectroscopy.⁶ The technique depends on the selection of a subgroup of molecules with a small range of velocities near $v=0$ using a narrow linewidth laser source.⁶ In particular, saturation spectroscopy is based on the selective saturation of an inhomogeneously broadened transition. A laser source "burns a hole" into the population distribution of the absorbing state by exciting a corresponding peak in the same velocity component in the upper state. Such a hole can be detected by frequency scanning a second laser source through resonance with the first source and monitoring the attenuation of the transmitted beam.

If the output from a single laser is split into two beams which are arranged to counter-propagate in the same media (see Figure 2), then two holes will be burned symmetrically about the line center. The two beams interact with the same velocity groups only when the laser is tuned to line center. The absorption of one of the beams (probe beam) will diminish at line center if the intensity of the second beam (pump beam) is sufficiently intense (near saturation) to alter the population distribution in the absorbing state. This dip in the probe beam absorption at line center due to the counter-propagating pump beam is termed the *Lamb Dip*. One technique for using this Lamb Dip to perform sub-Doppler spectroscopy involves modulating the amplitude of the pump beam and monitoring the modulated portion of the transmitted probe beam. A non-zero signal is obtained only when the two beams interact with the same velocity group ($v=0$) in the region where the two beams are overlapped. The observed linewidth is reduced to the homogeneous (Lorentzian) limit. Such sub-Doppler spectroscopy has been demonstrated for molecular iodine,⁷ and other atomic and molecular species.⁶



In the current paper we demonstrate a novel variant of the laser saturation spectroscopy which retains the Doppler-limited lineshape, but provides spatial resolution. A schematic diagram for these experiments is shown in Figure 3. By arranging the pump and probe beam to cross each other with a small, but finite angle, the two beams can be made to simultaneously interact only with a small volume of gas. Since the two beams propagate in the same direction, they always interact with the same velocity group, and the full Doppler profile is retained. The Doppler profile can then be utilized to determine the translational temperature for the absorbing medium in the crossing volume. The width, Δv_D , (FWHM) for a single Doppler broadened line is related to the temperature, T , according to the relationship:



$$\Delta v_D = \sqrt{\frac{8kT \ln 2}{Mc^2}} v_o \quad (1)$$

where v_o is the line center and M is the mass of the absorbing atom or molecule. By fitting the theoretical spectrum to the experimental spectra, using the temperature as the fitting parameter, one can determine the local temperature of the absorbing medium.

Molecular iodine, I_2 , is a convenient candidate for laser saturation spectroscopy in the COIL device. The saturation intensity is low and many ro-vibrational transitions of the B-X system are accessible in the red portion of the visible spectrum. The near coincidence of several rotational features, possible from different vibrational levels may aid in temperature determination, as the intensities of the rotational features are given by the statistical distribution:

$$\frac{N(J)}{N_{tot}} = \left(\frac{hcB_v}{kT} \right) (2J + 1) e^{-J(J+1)hcB_v/kT} \quad (2)$$

where B_v is the rotational constant and J is the rotational quantum number.

In the present study, a Coherent model 899 ring dye laser pumped by a Spectra Physics Model 2080 Ar^+ laser at 514.5 nm was used as the laser excitation source. Exciton Rhodamine 590 dye was used to cover the spectral region 16260.16–18083.18 cm^{-1} . The intensity of the transmitted probe beam was monitored with a Hamamatsu S2281 silicon photodiode. The side fluorescence was detected with a Burle Photomultiplier Tube model C31034A02. The laser beam was amplitude modulated with a Model SR540 mechanical chopper at 0 – 4000 Hz and the phase sensitive detection was accomplished using a Stanford Research Systems model SR850 lock-in amplifier. A static glass cell (41.5 cm long) was evacuated to < 16 mTorr using a Alcatel 2015 C2 rotary vane pump. Iodine and added buffer gas pressures were monitored with MKS pressure transducers: MKS Model 390HA for < 1 Torr and a MKS Model 690A for 1 to 1000 Torr; both utilizing a MKS Type 270 signal conditioner.

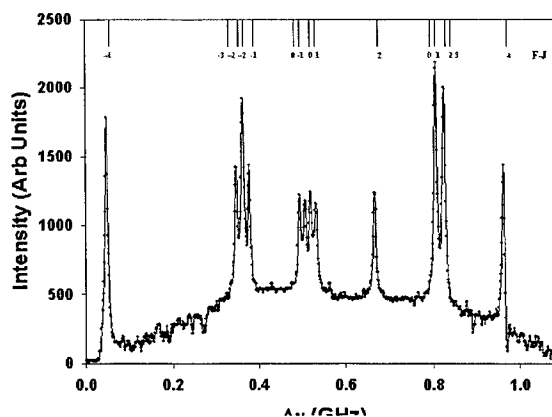
3. RESULTS

3.1 Hyperfine Spectrum

The sub-Doppler laser saturation spectrum of the isolated (171) P(70) line of the $I_2 X^1\Sigma_g^+ - B^3\Pi(0_u^+)$ transition at $\nu=17339.8187 \text{ cm}^{-1}$ is shown in Figure 4. The spectrum is composed of a set of either 15 or 21 hyperfine spectral components, depending on the parity of the rotational state. The hyperfine components are labeled according to value of F-J, as discussed below.

The Hamiltonian for the nuclear electric quadrupole interaction is:

$$\hat{H}_{NEQ} = -eQq \left(\frac{3(\bar{I}_1 \cdot \bar{J})^2 + \frac{3}{2}(\bar{I}_1 \cdot \bar{J}) - |\bar{I}_1|^2 |\bar{J}|^2}{2(2J+3)(2J-1)I_1(2I_1-1)} + \frac{3(\bar{I}_2 \cdot \bar{J})^2 + \frac{3}{2}(\bar{I}_2 \cdot \bar{J}) - |\bar{I}_2|^2 |\bar{J}|^2}{2(2J+3)(2J-1)I_2(2I_2-1)} \right) \quad (3)$$



where Q is the electric quadrupole moment, q_J is the average E-field gradient along the J direction, e is the electron charge, J is the sum of the spin and orbital angular momentum of the molecule, and $I_1=I_2=5/2$ is the atomic iodine nuclear spin angular momentum. The Hamiltonian for the nuclear magnetic dipole interaction is

$$H_m = \mu \frac{G}{I_1} (\vec{I}_1 \cdot \vec{J}) \quad (4)$$

where $\mu G/I_1$ is the spin rotation coupling constant. Finding energy eigenvalue solutions to the Hamiltonian involves the diagonalization of a nontrivial matrix. However, approximate solutions can be found for $J \gg 1$ of the form:⁸

$$E = E_{NEQ} + E_M$$

$$E_{NEQ} \cong -\frac{eQq}{8I_1(2I_1-1)} \left\{ (M_1^2 + M_2^2) + \frac{3}{J} M_1 \left[M_1(M_1+1) - I_1(I_1+1) + \frac{1}{2} \right] + \frac{3}{J} M_2 \left[M_2(M_2+1) - I_1(I_1+1) + \frac{1}{2} \right] - 2I_1(I_1+1) \right\} \quad (5)$$

$$E_M \cong \frac{\mu G}{I_1} (M_1 + M_2) J$$

Table I provides an evaluation of equation (5) for $v'=21, J'=116$ line using the values $eQq=-2900$ MHz and $G/I_1=0.049$ MHz. For $I_1=I_2=5/2$, the possible values from the projection along the internuclear axis are $-5/2 \leq M_1, M_2 \leq +5/2$. The Pauli exclusion principle requires the total wave function of a homonuclear diatomic molecule with a half integer nuclear spin remain antisymmetric under an exchange of the nuclei. As a consequence the $M_1 = M_2$ combinations are forbidden for J' =odd, but included for J' =even. The relative line positions for $v'=21$ for a broad range of rotational states based on the approximate solution of equation (5) is provided in Figure 5.

Table I
Hyperfine splitting for $v'=21, J'=116$.

M_1	M_2	F-J	$E_{NEQ}+E_m$
2.5	2.5	5 122	755.989
2.5	1.5	4 121	307.820
2.5	0.5	3 120	87.375
2.5	-0.5	2 119	89.078
2.5	-1.5	1 118	307.352
2.5	-2.5	0 117	736.619
1.5	1.5	3 120	-140.349
1.5	0.5	2 119	-360.794
1.5	-0.5	1 118	-359.091
1.5	-1.5	0 117	-140.817
1.5	-2.5	-1 116	288.450
0.5	0.5	1 118	-581.238
0.5	-0.5	0 117	-579.535
0.5	-1.5	-1 116	-361.262
0.5	-2.5	-2 115	68.005
-0.5	-0.5	-1 116	-577.832
-0.5	-1.5	-2 115	-359.559
-0.5	-2.5	-3 114	69.708
-1.5	-1.5	-3 114	-141.286
-1.5	-2.5	-4 113	287.981
-2.5	-2.5	-5 112	219.592

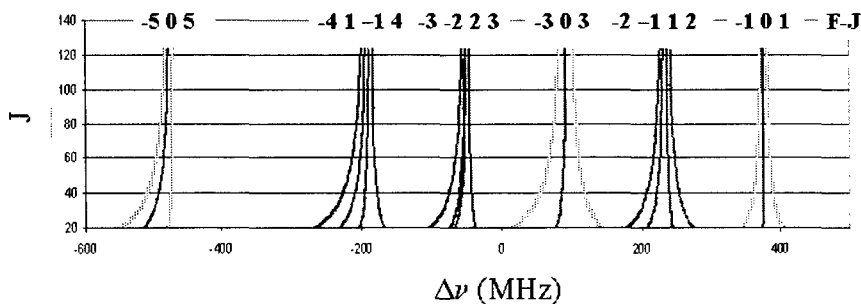


Figure 5. Predicted hyperfine splitting within $v'=21$.

3.2 Pressure Broadening

The hyperfine components are well represented by pressure dependent Lorentzian lineshapes. In Figure 6, the hyperfine spectrum is shown for two argon buffer gas pressures. Significant broadening is evident for low pressures. A set of Lorentzian lineshapes with common widths have been fit to the type of hyperfine data of Figure 6 for a variety of argon buffer gas pressures where the I2 pressure was fixed at .1635 Torr. The resulting linewidths are shown in Figure 7. The fit includes a Gaussian baseline, which is described below in the velocity cross-relaxation discussion.

The intercept in Figure 7 indicates a zero-pressure broadening of 9.40 ± 0.16 MHz, which corresponds to natural broadening with a lifetime of $0.67 \mu s$. The collisionless lifetime ($1/\tau_0 = 1/\tau_{rad} + 1/\tau_{nr}$) for this state is $\tau_0 = 1.08-1.14 \mu s$.⁹

The slope in Figure 7 provides a pressure broadening rate of 8.14 ± 0.30 MHz/Torr. This result is somewhat higher than the value of 6.6 MHz/Torr reported from Doppler limited absorption studies,¹⁰ and significantly larger than the (v,J) dependent rates of 0.31 – 2.96 MHz/Torr reported from fluorescence depolarization studies.¹¹ Further studies are in progress to examine the pressure broadening rates for a wide variety of collision partners.

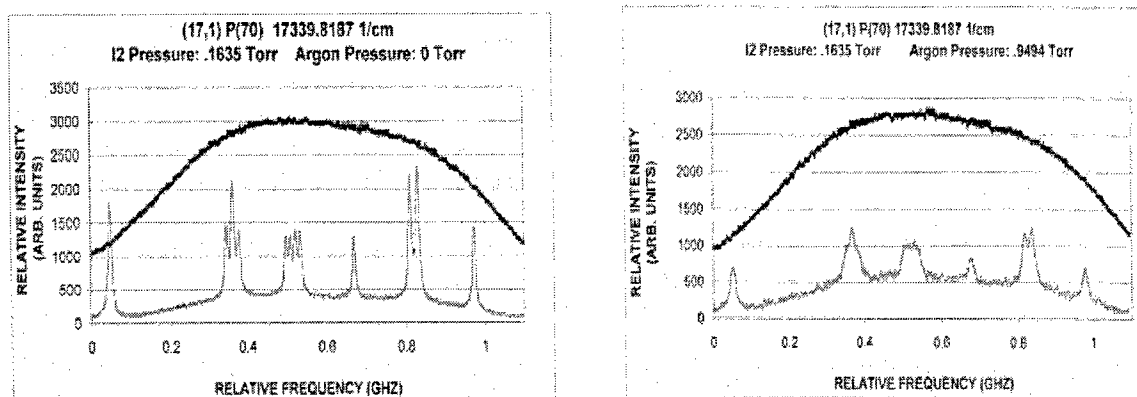


Figure 6. Pressure broadened hyperfine spectrum for the (17,1) P(70) line.

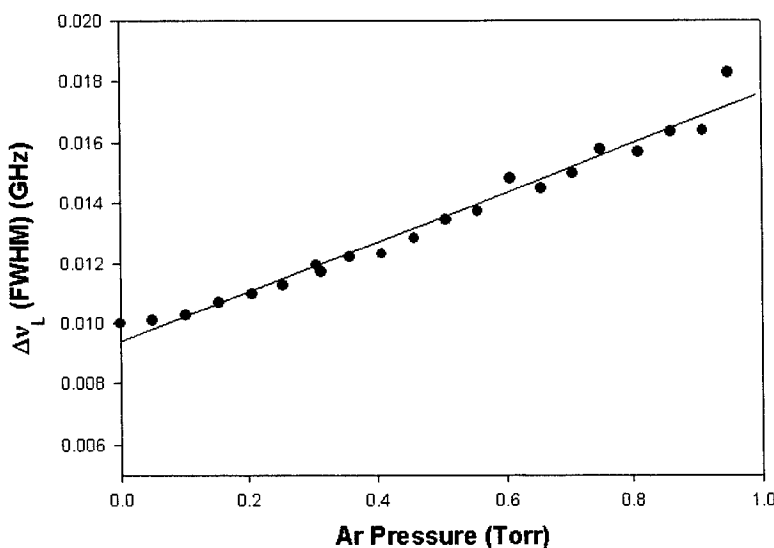


Figure 7. Pressure broadening rate for (17,1) P(70) line with argon collision partner.

Pressure broadening at higher pressures can be obtained from the laser excitation spectra. Figure 8 illustrates the side fluorescence intensity as a function of laser frequency and represents the convolution of 15 Voigt broadened hyperfine levels. To extract the pressure broadening rates, a fit of the hyperfine lines is performed. The spectrum of Figure 8 is fit to the convolved lineshape function:

$$g_V(\nu) = \sum_{i=1}^{15 \text{ or } 21} \text{Voigt}(\nu; I_i, \nu_{oi}, \Delta\nu_D, \Delta\nu_L) e^{-c \sum_{i=1}^{15 \text{ or } 21} \text{Voigt}(\nu; I_i, \nu_{oi}, \Delta\nu_D, \Delta\nu_L)} + a + b\nu \quad (6)$$

where a and b represent the background baseline, c is required to model the self absorption of the pump beam by the I_2 gas, the relative intensities of the hyperfine components, I_i , are constrained by their statistical weights, $2F+1$, ν_{oi} is the

hyperfine component line center positions as determined from the sub-Doppler spectrum, Δv_D is the common Doppler width (FWHM), and Δv_L is the common Lorentzian width (FWHM). The fit shown in Figure 8 was performed with the Doppler width constrained by the known sample temperature at $T=292.6$ K, and the Lorentzian width defined by the intercept in Figure 7 and the self broadening rate of $\gamma_{I_2} = 8$ MHz/Torr.¹² A complete analysis of these laser excitation spectra lineshapes at high pressure for a wide variety of collision partners is in progress. A fit to the I_2 side fluorescence broadened by Ar buffer gas is shown in Figure 9 where the Doppler width is constrained as mentioned and the Lorentzian is defined additionally by the Ar pressure broadening rate from Fig. 7.

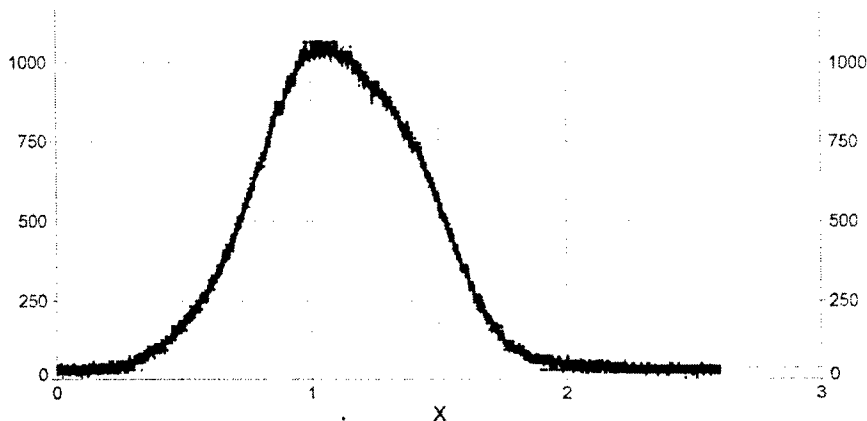


Figure 8. Laser excitation spectrum of (17,1) P(70) line at 36.5 mTorr I_2 .

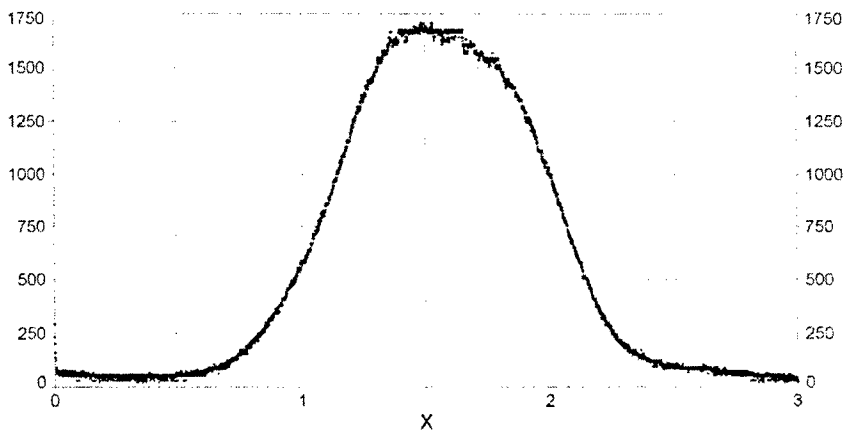


Figure 9. Laser excitation spectrum of (17,1) P(70) line at 163.5 mTorr I_2 and 3.1 Torr Ar.

3.3 Velocity Cross-Relaxation

The sub-Doppler laser saturation spectra exhibit a broader feature upon which the hyperfine structure is superimposed. The amplitude of this feature depends on rotational level, J , pressure, and modulation frequency, as shown in Figure 10. Two, closely spaced rotational lines with significantly different rotational states are overlapped in these 2 GHz scans. The broader feature is much more intense for the lower rotational level. The intensity of the broad feature relative to the intensity of the hyperfine resolved components decreases with modulation frequency (as shown in Figure 10b) and total pressure. Similar affects have been observed previously and attributed to velocity cross-relaxation dynamics.⁷

To further illustrate these collisional dynamics, consider the following example. An I_2 non-zero velocity group, v_g , interacts with the pump beam and then suffers a collision that converts the velocity group to $-v_g$. The probe beam is then in resonance with the new velocity group, and as long as the collision occurs during the same modulation cycle, the probe laser intensity is correlated with chopping frequency. Since such collisions can occur for any velocity group, v_g , a broad feature with Gaussian shape is obtained. At higher pressures and lower modulation rates, more collisions occur and contribute to a more intense feature. Apparently, the dynamics are dominated by rotationally inelastic collisions, yielding a strong dependence on rotational state. Multiple collisions would be required for R-T events, to return the population to the initial state and contribute to the observed lineshape.

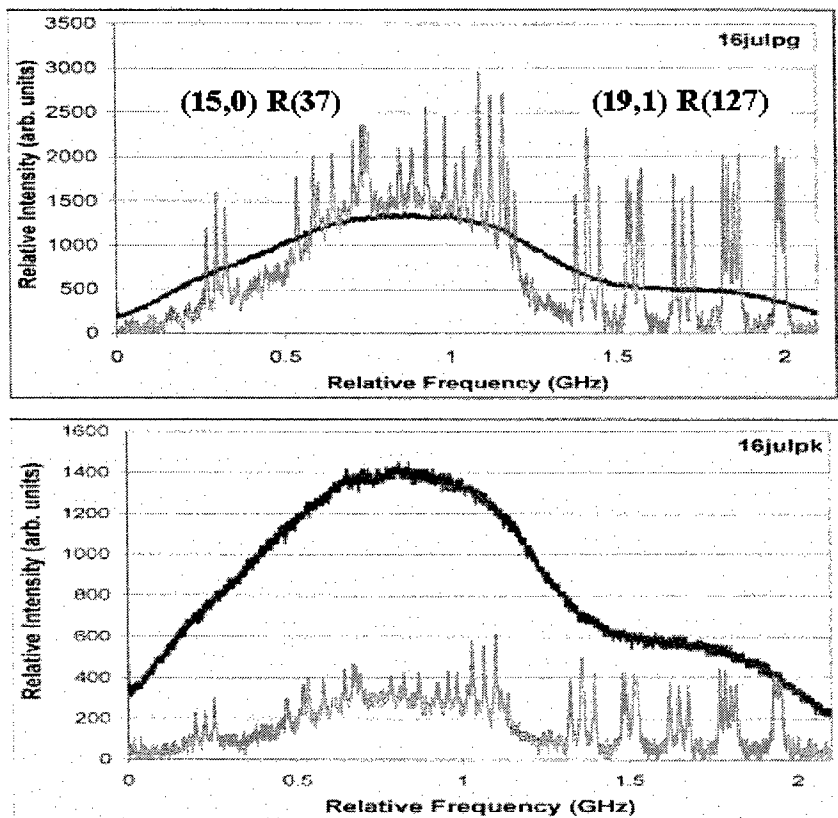


Figure 10 Upper spectrum taken at a chopping frequency of 1000 Hz. Lower spectrum taken at a chopping frequency of 3754 Hz.

3.3 Spatially-Resolved Temperature Diagnostic

The Doppler limited laser saturation spectrum for the (17,1) P(70) line using the apparatus described in Figure 3 is shown in Figure 11.¹³ For these studies, a static I_2 cell with differential heating was employed. The hot end of the cell was maintained at $T = 523$ K. The pump and probe beams were co-propagated with a small crossing angle of 3.8 degrees, resulting in a crossing volume of 12 mm^3 . Three spectra were recorded; near the hot end, in the center and near the colder end of the 0.5" diameter by 6" length cell. The width of the observed lineshapes increases with increasing cell temperature, establishing the feasibility of extracting spatially resolved temperatures. The lineshape studies discussed above are essential to extracting accurate temperatures.

Figure 12 predicts the lineshapes for temperatures in increments of 50 K from 50 - 400K. The sensitivity of the diagnostic is improved at lower temperatures, and we are pursuing the application of the technique in a supersonic

expansion as discussed below. The uncertainty in extracted temperatures may be further enhanced by using several closely spaced lines associated with different rotational levels as shown in Figure 10. The rotational Boltzmann distribution of equation (2) can be used to further constrain the temperature.

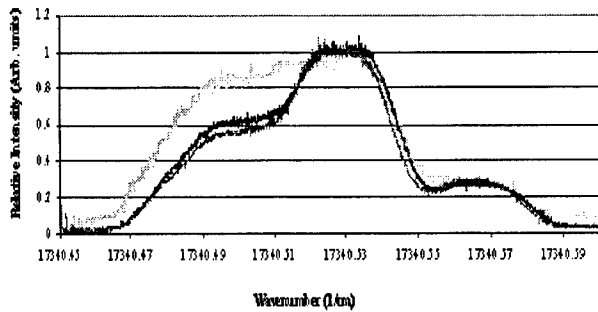


Figure 11. Doppler-limited saturation spectra at three locations in a differentially heated cell.

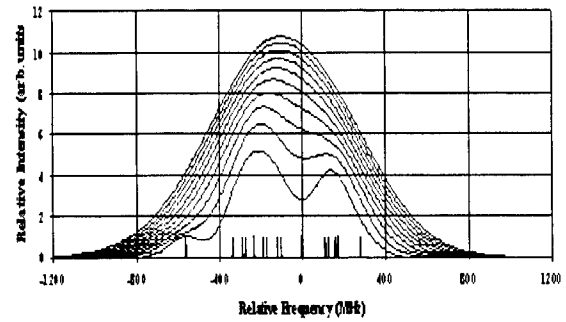


Figure 12. Predicted Doppler-limited saturation spectra at T=50 – 400 K in 50K increments.

A Laval nozzle designed by the Air Force Research Laboratory will be used to simulate the conditions in a COIL supersonic nozzle. The Laval nozzle produces a flow at the exit with constant Mach number.¹⁴ A schematic of the nozzle is shown in Figure 12. A diffuser is located after the gas inlet to establish a near-zero net hydrodynamic velocity. After the diffuser, there is a convergent section where the flow begins to accelerate and then passes through the throat, to reach its maximum velocity. The Mach number at any point in the along the nozzle can be obtained from the expression for the area ratio:¹⁴

$$\frac{A}{A^*} = \frac{1}{M} \left[\left(\frac{2}{k+1} \right) \left(1 + \frac{k-1}{2} M^2 \right) \right]^{\frac{k+1}{2(k-1)}} \quad (7)$$

where A^* is the cross-sectional area of the throat, $k=c_p/c_v$ is the ratio of the heat capacity at constant pressure to the heat capacity at constant volume, and M is the Mach number. At the throat, the Mach number is 1. Assuming the flow is accelerated to a uniform Mach number, the drop in temperature and pressure can be computed from:¹⁴

$$\frac{T_o}{T} = 1 + \frac{k-1}{2} M^2, \quad (8)$$

and

$$\frac{p_o}{p} = \left(1 + \frac{k-1}{2} M^2 \right)^{\frac{k}{k-1}}, \quad (9)$$

where T_o , and p_o are the temperature and pressure in the pre-expansion stagnation region. Assuming the stagnation temperature $T_o=298.15$ K, the temperature at the point where the nozzle widens to 0.7 cm is $T \cong 183$ K .

4. CONCLUSIONS

A novel variant of laser saturation spectroscopy to diagnose the temperature in the supersonic nozzle of a Chemical Oxygen-Iodine Laser has been demonstrated. Accurate temperature measurements require high signal-to-noise spectral lineshapes and detailed characterization of hyperfine line positions, pressure broadening rates, and self-absorption. Initial studies of the sub-Doppler lineshapes have been reported. The sub-Doppler spectra exhibit features related to

velocity cross-relaxation which may be used to study rotationally inelastic collisions. The extension of this technique to supersonic flows is in progress.

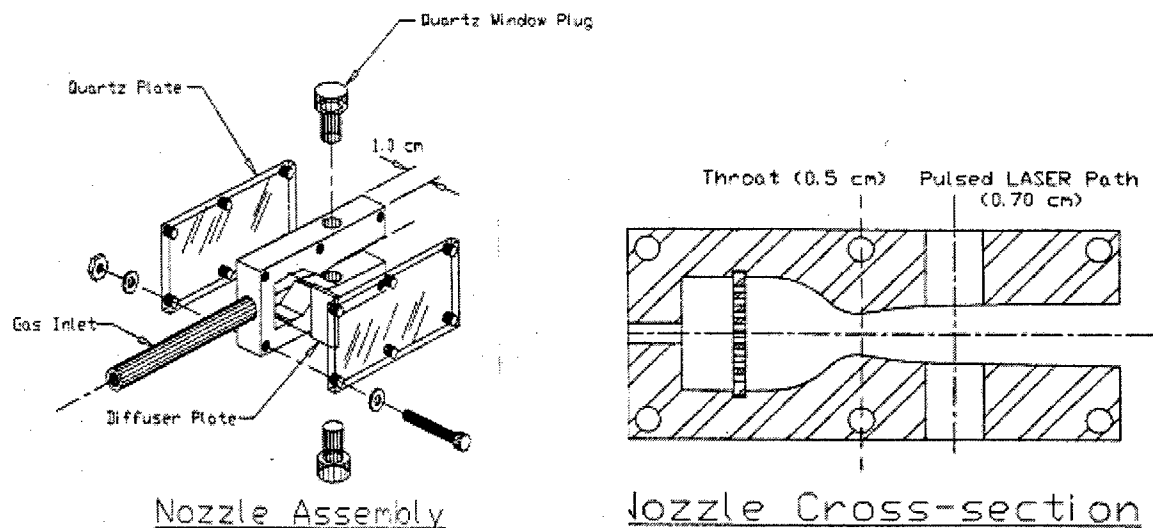


Figure 13. Laval nozzle for demonstration of spatially resolved temperature measurement at low temperatures.

REFERENCES

1. McDermott, W.E., N.R. Pchelkin, D.J. Benard, and R.R. Bousek, "An Electronic Transition Chemical Laser," *App. Phys. Lett.* **32** 469 (1978).
2. N. Bloembergen and C.K.N. Patel (Co-chairs, APS Study Group), *Rev. Mod. Phys.* **59**, S1 (1987).
3. K.A. Truesdell, S.E. Lamberson, and G.D. Hager, *AIAA* **92**, 3003 (1992).
4. P.V. Avizonis, G. Hasen, and K.A. Truesdell, *SPIE* **1225**, 448 (1990).
5. P.B. Keating, C.A. Helms, B.T. Anderson, T.L. Rittenhouse, K.A. Truesdell, and G.D. Hager, "Two-Dimensional Gain and Cavity Temperature Maps of a Small-Scale Supersonic COIL," in *Proceedings of the International Conference on Lasers '96*, Ed. Pp 194-201, V.J. Corcoran and T.A. Goldman, editors, STS Press, McLean, VA, 1997.
6. Demtroder, Wolfgang. *Laser Spectroscopy*, Berlin: Springer, 1998.
7. Morinaga, A. "Cross-relaxation Effects on the Saturation of the Visible Absorption Lines of the Iodine Molecule," *J. Opt. Soc. Am. B*, **4** (6): 906-909 (June 1987).
8. Levenson, M. D., and A.L. Schawlow, "Hyperfine Interactions in Molecular Iodine," *Physical Review A*, **6** 10-20 (July 1972).
9. Capelle, Gene A., and H.P. Broida, "Lifetimes and Quenching Cross Sections of $I_2(B^3\Pi_{Ou}^+)$," *The Journal of Chemical Physics*, **58** 4212-4222 (15 May 1973).
10. S.V. Kireev, S.L. Shnyrev, and Yu.P. Zaspa, *Optics and Spectroscopy*, **78** 550 (1995).
11. M. Berjot, L. Bernard, and T. Theophanides, *Can J Spectrosc* **18** 128 (1973).
12. Sorem, M.S., and A.L. Schawlow, "Saturation Spectroscopy in Molecular Iodine by Intermodulated Fluorescence," *Optics Communications*, **5** 148-151 (1972).
13. Myers Jr., James W. *Spatially Resolved Temperature Determination in I_2 Gas Using Doppler-Limited Saturation Spectroscopy*. MS Thesis, AFIT/GAP/ENP/00M-03. Graduate School Engineering and Management, Air Force Institute of Technology (AU), Wright-Patterson AFB OH, March 2000.
14. Shapiro, Ascher H. *The Dynamics and Thermodynamics of Compressible Fluid Flow, Vol. I*. New York: John Wiley & Sons, 1953, p.86.